Hyperchaotic behaviors, optimal control, and synchronization of a nonautonomous cardiac conduction system

Dumitru Baleanu[1,2,3], Samaneh Sadat Sajjadi[4], Jihad H. Asad[5], Amin Jajarmi[6,7*] and Elham Estiri[4]

*Correspondence: a.jajarmi@ub.ac.ir
[6]Department of Electrical Engineering, University of Bojnord, P.O. Box, 94531-1339, Bojnord, Iran
[7]Department of Mathematics, Near East University TRNC, Mersin 10, Nicosia, Turkey
Full list of author information is available at the end of the article

Abstract

In this paper, the hyperchaos analysis, optimal control, and synchronization of a nonautonomous cardiac conduction system are investigated. We mainly analyze, control, and synchronize the associated hyperchaotic behaviors using several approaches. More specifically, the related nonlinear mathematical model is firstly introduced in the forms of both integer- and fractional-order differential equations. Then the related hyperchaotic attractors and phase portraits are analyzed. Next, effectual optimal control approaches are applied to the integer- and fractional-order cases in order to overcome the obnoxious hyperchaotic performance. In addition, two identical hyperchaotic oscillators are synchronized via an adaptive control scheme and an active controller for the integer- and fractional-order mathematical models, respectively. Simulation results confirm that the new nonlinear fractional model shows a more flexible behavior than its classical counterpart due to its memory effects. Numerical results are also justified theoretically, and computational experiments illustrate the efficacy of the proposed control and synchronization strategies.

Keywords: Nonautonomous system; Cardiac conduction; Fractional calculus; Hyperchaos control; Synchronization

1 Introduction

Chaos is one of the most prominent features of nonlinear dynamical systems whose state variables are highly dependent on its initial conditions. This dependency leads to the divergent behavior of such systems, the fact which reveals the great importance of detailed study regarding chaotic phenomena. Because of the wide appearance of chaos in different fields such as acoustic and secure communications, physics, biology, economy, etc., many scientists and mathematicians have been dealing with controlling and synchronizing chaotic dynamical systems extensively [1–5]. In [6], using scalar transmitted signal, a new systematic approach was designed to synchronize a class of hyperchaotic systems. In [7], an optimal control scheme was presented for chaotic/hyperchaotic systems by formulating a linear feedback control problem. In [8], two identical hyperchaotic systems were synchronized using a nonlinear control technique, and the stability of the proposed algo-

rithm was proved by using both Lyapunov and Cardono methods. In [9], a parameter observer was investigated in order to identify unknown parameters in hyperchaotic systems, which is needed to design the state-feedback controller. The authors in [10] controlled and synchronized chaotic systems using state-dependent Riccati equations. In [11], the chaotic Lorenz and hyperchaotic Chen systems were considered in the presence of parameter uncertainty and controlled using an adaptive dual synchronization controller. In [12], a terminal sliding model control was applied to the chaotic Chen and hyperchaotic Lorenz systems; then using an adaptive terminal sliding mode control, the authors achieved the aim of synchronization. In [13], considering the stability theory of Lyapunov, the authors synchronized three nonidentical systems of different dimensions.

Recently, the investigation of complex behaviors in biology such as chaos has attracted the attention of biomedical engineers due to the unpredictable characteristics of biological systems [14–16]. In [17], after investigating chaos in the mathematical model of tumor, the authors controlled the chaotic behavior of tumor cells using a non-feedback loop. In [18], the authors designed an optimal drug delivery schedule for the chaotic behavior of tumor cells by minimizing Hamiltonian function; then in [18], they controlled the same system considering uncertainty in the chaotic model of cancer. In [19], the authors discussed the chaotic behavior of Lotka–Volterra biological systems; then they applied an effective control scheme for the purpose of synchronization.

In recent years, a noticeable number of researches have used fractional-order systems due to their memory-oriented features, which makes them more realistic compared to their integer-order counterparts [20–30]. Also, it is very practical to consider chaos and hyperchaos in such systems in order to simulate the complex behavior of real-world phenomena. In [31], the authors synchronized the chaotic behavior of fractional-order systems according to the stability conditions and using a feedback control method. In [32], a control approach and a synchronization strategy were extended for three fractional chaotic maps. In [33], a newly introduced fractional hyperchaotic system was controlled and synchronized by choosing an appropriate Lyapunov function and using state-feedback control computation. In [34], the authors designed a linear feedback controller for the purpose of chaos control; then a control scheme was used to synchronize the chaotic behavior of two identical biological snap oscillators.

Biochemical oscillators play a vital role in biological sciences; for instance, a cardiac conduction system can be considered as a network of self-stimulated elements like sinus or SA node (the first pacemaker), atrioventricular node (AV node), and His–Purkinje system. Because these elements show oscillatory behavior, they can be modeled as nonlinear oscillators. In addition, an external stimulation is entered into the system with regard to the oscillator frequency, which is interpreted as a nonautonomous term in the nonlinear dynamical system [35]. Besides, stabilization techniques have been used to overcome the chaotic oscillations of biological systems. Moreover, synchronization schemes aim to suppress the situation when a short or long spatial scale difference occurs between oscillators. Therefore, the employment of appropriate control actions is essential to synchronize two identical chaotic systems which are highly sensitive to initial conditions. Hence, the problems of stabilization and synchronization have been of great importance from both biological and mathematical points of view. Based on the above-mentioned arguments, this paper introduces an integer-order model as well as a new fractional-order formal-

ism for a nonautonomous cardiac conduction system. The main contributions of the new achievements in this paper are summarized as follows:

- In this paper, we analyze the hyperchaotic behaviors of the new models and discuss the stability of their equilibrium point.
- We stabilize the hyperchaotic behaviors of the integer-order model as well the fractional-order formalism by using optimal controllers based on Pontryagin's maximum principle (PMP).
- We also synchronize two identical hyperchaotic oscillators in the frameworks of both classical and fractional equations by applying an adaptive controller and an active compensator, respectively.
- Finally, we present some simulations in order to verify the theoretical analysis.

To the best of our knowledge, the mathematical modeling, hyperchaos control, and synchronization strategies presented in this paper for a cardiac conduction system are new and comprise some valuable information, the fact which makes the obtained results in this paper noteworthy from both biological and mathematical points of view.

The remainder of this paper is organized as follows. In Sect. 2, an integer- and a fractional-order models are introduced for a nonautonomous cardiac conduction system. In Sect. 3, both new models are stabilized by using optimal control strategies. Afterwards, we employ an adaptive control scheme and an active controller for the aim of synchronization in the sense of classical and fractional frameworks, respectively. Finally, some concluding remarks and discussions are stated in the last section.

2 Mathematical model

In this section, the mathematical model of a cardiac conduction system, introduced in [35], is investigated in the sense of both classical and fractional frameworks. As there exists a noticeable similarity between the behaviors of classical Van der Pol oscillators and the qualitative features of some nonlinear biological systems, the Van der Pol equations play a key role in the modeling and simulation of biological oscillatory systems such as heart and lungs in a human body. The Van der Pol equations, which were firstly introduced in [36], are defined as

$$\begin{cases} \dot{f}_1 = f_2, \\ \dot{f}_2 = -\alpha(f_1^2)f_2 - \beta f_1 + \gamma \cos(\omega t), \end{cases} \tag{1}$$

in which the chaotic or non-chaotic behaviors depend on the values of the parameters α, β, and γ. In the following subsections, we introduce two mathematical extensions of Eq. (1) in the frameworks of integer- and fractional-order calculus to investigate the hyperchaotic cardiac oscillatory behaviors.

2.1 Integer-order case

If we consider the heart in a body as a nonlinear oscillatory system, then the cardiac conduction must be taken into account as a combination of two subsystem oscillators, which refer to arterial sinus node (SA) and atrioventricular node (AV). Also, the third oscillation is worth to be incorporated to simulate complex QRS, which indicates His−Purkinje complex in a biological way. Thus, three oscillators work in combination in order to replicate the heart functionality. As a result, the following extended integer-order model can

Table 1 The parameter values of model (2)

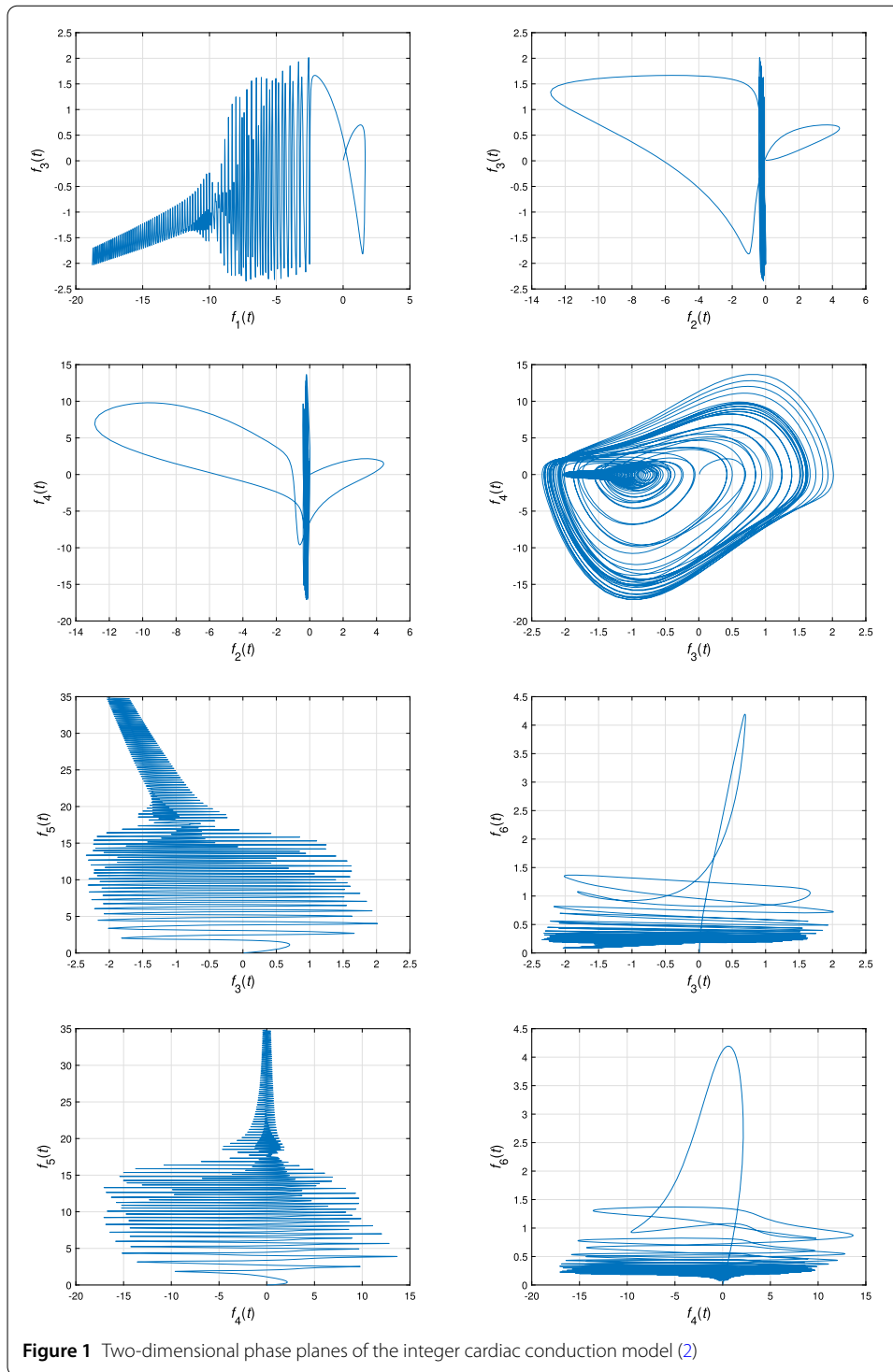| Parameter	Description	Value
α_1	Limit cycle in the phase portrait of (f_1, f_2)	5
α_2	Limit cycle in the phase portrait of (f_3, f_4)	4.75
α_3	Limit cycle in the phase portrait of (f_5, f_6)	4.75
β_1	Frequency of SA node	6
β_2	Frequency of AV node	30
β_3	Frequency of His–Purkinje complex	1.7
γ_1	Modeling constant coefficient	5
γ_2	Modeling constant coefficient	6
γ_3	Modeling constant coefficient	4
r_{13}	Coupling coefficient between SA node and AV node	2
r_{15}	Coupling coefficient between SA node and His–Purkinje complex	3
r_{31}	Coupling coefficient between AV node and SA node	1
r_{35}	Coupling coefficient between AV node and His–Purkinje complex	2
r_{51}	Coupling coefficient between His–Purkinje complex and SA node	7
r_{53}	Coupling coefficient between His–Purkinje complex and AV node	5

describe a cardiac conduction system including six types of variables [35]:

$$
\begin{cases}
\dot{f}_1 = f_2, \\
\dot{f}_2 = -\alpha_1(f_1^2 - 1)f_2 - \beta_1 f_1 + \gamma_1 \cos(\omega t) + r_{13}(f_1 - f_3) + r_{15}(f_1 - f_5), \\
\dot{f}_3 = f_4, \\
\dot{f}_4 = -\alpha_2(f_3^2 - 1)f_4 - \beta_2 f_3 + \gamma_2 \cos(\omega t) + r_{31}(f_3 - f_1) + r_{35}(f_3 - f_5), \\
\dot{f}_5 = f_6, \\
\dot{f}_6 = -\alpha_3(f_5^2 - 1)f_6 - \beta_3 f_5 + \gamma_3 \cos(\omega t) + r_{51}(f_5 - f_1) + r_{53}(f_5 - f_3),
\end{cases}
\tag{2}
$$

in which the pairs (f_1, f_2), (f_3, f_4), and (f_5, f_6) show SA, AV, and His–Purkinje oscillators, respectively. In addition, the parameters β_1, β_2, and β_3 are the frequencies of SA node, AV node, and His–Purkinje complex, respectively, and r_{ij} shows the coupling coefficient between relevant nodes. The stabilities of limit cycles in the phase portrait of (f_1, f_2), (f_3, f_4), and (f_5, f_6) are denoted by α_1, α_2, and α_3, respectively. The description of all parameters and their values are given in Table 1. Considering the parameter values as mentioned in Table 1 as well as the initial conditions $F(0) = (f_1(0), f_2(0), f_3(0), f_4(0), f_5(0), f_6(0)) = (0.01, 0.01, 0.01, 0.01, 0.01, 0.01)$, we sketch the simulation results of the aforementioned equations in Figs. 1–2 including two- and three-dimensional phase portraits. Note that the parameters and the initial values are selected such that the considered system depicts hyperchaotic behaviors. In order to show that the nonlinear oscillator (2) is dissipative, i.e., all trajectories narrow down to zero, we consider the vector N and its divergence as follows:

$$
N = \begin{bmatrix} n_1 \\ n_2 \\ n_3 \\ n_4 \\ n_5 \\ n_6 \end{bmatrix} = \begin{bmatrix} f_2 \\ -\alpha_1(f_1^2 - 1)f_2 - \beta_1 f_1 + \gamma_1 \cos(\omega t) + r_{13}(f_1 - f_3) + r_{15}(f_1 - f_5) \\ f_4 \\ -\alpha_2(f_3^2 - 1)f_4 - \beta_2 f_3 + \gamma_2 \cos(\omega t) + r_{31}(f_3 - f_1) + r_{35}(f_3 - f_5) \\ f_6 \\ -\alpha_3(f_5^2 - 1)f_6 - \beta_3 f_5 + \gamma_3 \cos(\omega t) + r_{51}(f_5 - f_1) + r_{53}(f_5 - f_3) \end{bmatrix},
\tag{3}
$$

$$
\nabla . N = \frac{\partial n_1}{\partial f_1} + \frac{\partial n_2}{\partial f_2} + \frac{\partial n_3}{\partial f_3} + \frac{\partial n_4}{\partial f_4} + \frac{\partial n_5}{\partial f_5} + \frac{\partial n_6}{\partial f_6} = -1.
\tag{4}
$$

Figure 1 Two-dimensional phase planes of the integer cardiac conduction model (2)

Thus, it can be concluded that all trajectories of the nonlinear biological oscillator (2) are likely to approach a chaotic attractor [37].

Remark 2.1 The dissipative property of a nonlinear biological system can be associated with its memory, the fact which is concluded from the dissipation feature of memory in real-world dynamical events [38].

Figure 2 Three-dimensional phase planes of the integer cardiac conduction model (2)
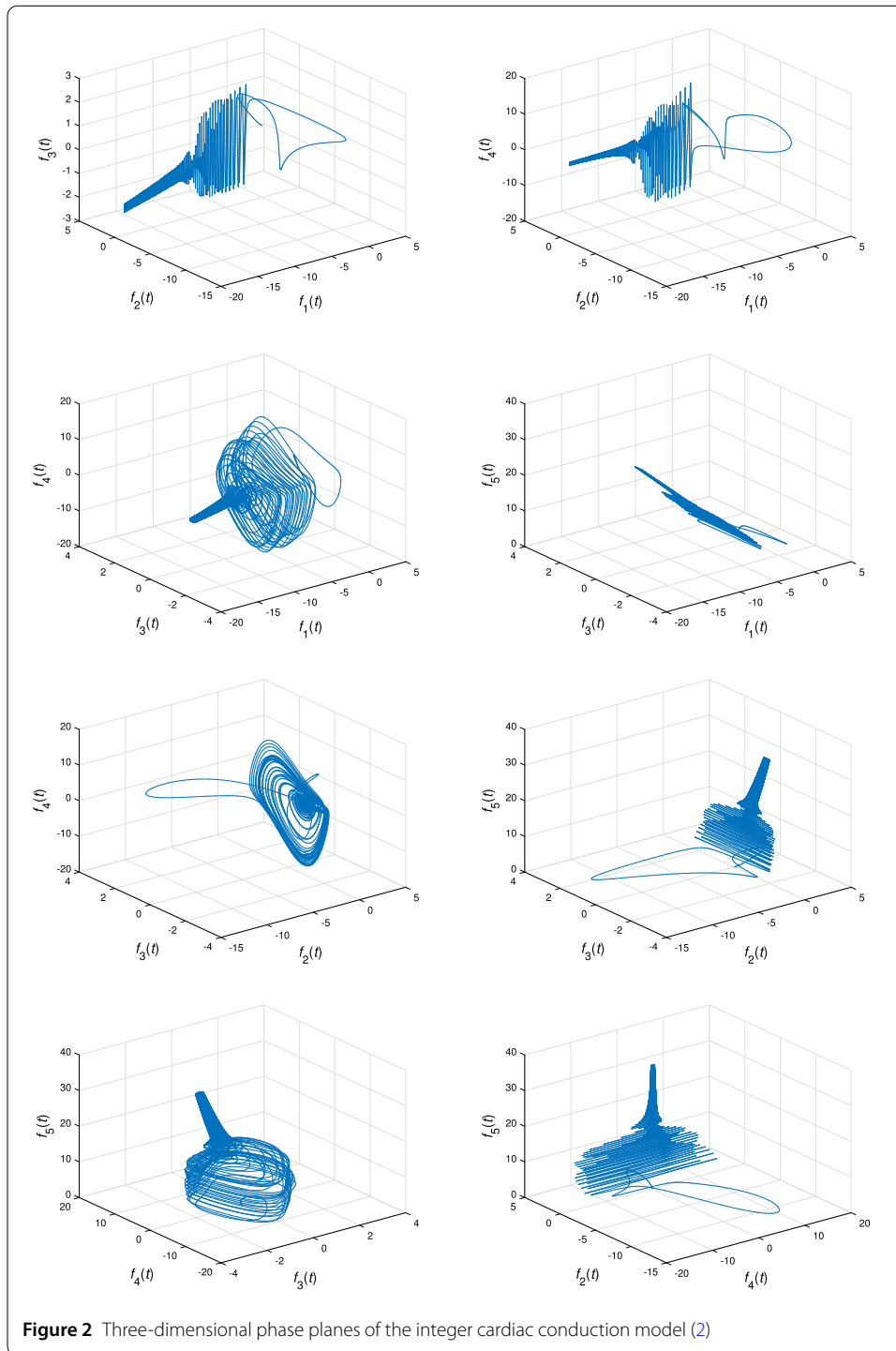
2.1.1 Equilibrium point and stability

By assuming the parameter values introduced in Table 1, we obtain the unique equilibrium of the hyperchaotic conduction model (2) as follows:

$$E = (2.042, 0, 0.084, 0, 0.93, 0)\cos(\omega t). \tag{5}$$

The the Jacobian matrix of system (2) is computed as

$$
J = \begin{bmatrix}
0 & 1 & 0 & 0 & 0 & 0 \\
j_{21} & -\alpha_1(f_1^2 - 1) & -r_{13} & 0 & -r_{15} & 0 \\
0 & 0 & 0 & 1 & 0 & 0 \\
-r_{31} & 0 & j_{43} & -\alpha_2(f_3^2 - 1) & -r_{35} & 0 \\
0 & 0 & 0 & 0 & 0 & 1 \\
-r_{51} & 0 & -r_{53} & 0 & j_{65} & -\alpha_3(f_5^2 - 1)
\end{bmatrix},
\tag{6}
$$

where

$$
\begin{aligned}
j_{21} &= -2\alpha_1 f_1 f_2 - \beta_1 + r_{13} + r_{15}, \\
j_{43} &= -2\alpha_2 f_3 f_4 - \beta_2 + r_{31} + r_{35}, \\
j_{65} &= -2\alpha_3 f_5 f_6 - \beta_3 + r_{51} + r_{53}.
\end{aligned}
\tag{7}
$$

Thus, the Jacobian matrix at E is acquired by

$$
J|_E = \begin{bmatrix}
0 & 1 & 0 & 0 & 0 & 0 \\
-1 & -20.8488\cos^2(\omega t) + 5 & -2 & 0 & -3 & 0 \\
0 & 0 & 0 & 1 & 0 & 0 \\
-1 & 0 & -28 & -0.0335\cos^2(\omega t) + 4.75 & -2 & 0 \\
0 & 0 & 0 & 0 & 0 & 1 \\
-4 & 0 & -5 & 0 & 7.3 & -4.1083\cos^2(\omega t) + 4.75
\end{bmatrix}.
$$
$$
\tag{8}
$$

As can be seen, the equilibrium point E and the related Jacobian matrix depend on time, so some eigenvalues of J depend on time, too, and they are sometimes positive. Therefore, E is an unstable equilibrium point.

2.2 Fractional-order case

Memory effects play an important role in the modeling and simulation of biological phenomena [39]. Due to this noticeable feature, in the following we introduce the fractional-order model of the hyperchaotic conduction system under consideration. To do so, first we define the left Caputo fractional derivative of $f_i(t)$ as follows:

$$
\begin{cases}
{}_0^C\mathscr{D}_t^{q_i} f_i(t) = \frac{1}{\Gamma(m_i - q_i)} \int_a^t f_i^{(m_i)}(\tau)(t - \tau)^{m_i - q_i - 1}\, d\tau, & m_i - 1 < q_i < m_i, \\
{}_0^C\mathscr{D}_t^{q_i} f_i(t) = f_i^{(m)}(t), & q_i = m_i,
\end{cases}
\tag{9}
$$

where q_i represents the order of fractional derivative, m_i is the first integer greater than q_i, and Γ is the gamma function. Then the fractional-order model of the considered biological system can be formulated by replacing the ordinary derivatives in Eq. (2) by the fractional-

order one defined in (9). Thus, the new fractional model is described by

$$
\begin{cases}
{}_{0}^{C}\mathscr{D}_{t}^{q_1} = f_2, \\
{}_{0}^{C}\mathscr{D}_{t}^{q_2} = -\alpha_1(f_1^2 - 1)f_2 - \beta_1 f_1 + \gamma_1 \cos(\omega t) + r_{13}(f_1 - f_3) + r_{15}(f_1 - f_5), \\
{}_{0}^{C}\mathscr{D}_{t}^{q_3} = f_4, \\
{}_{0}^{C}\mathscr{D}_{t}^{q_4} = -\alpha_2(f_3^2 - 1)f_4 - \beta_2 f_3 + \gamma_2 \cos(\omega t) + r_{31}(f_3 - f_1) + r_{35}(f_3 - f_5), \\
{}_{0}^{C}\mathscr{D}_{t}^{q_5} = f_6, \\
{}_{0}^{C}\mathscr{D}_{t}^{q_6} = -\alpha_3(f_5^2 - 1)f_6 - \beta_3 f_5 + \gamma_3 \cos(\omega t) + r_{51}(f_5 - f_1) + r_{53}(f_5 - f_3).
\end{cases}
\tag{10}
$$

Here, the interpretations of all variables and coefficients are the same as in the classic model (8); thus, the description of all parameters and their values are found again in Table 1.

The above-mentioned equations indicate the memory-oriented features of fractional calculus, which contains time from 0 to t as well as t in their derivatives. Considering the system parameters as introduced in Table 1 and the initial conditions $F(0) = (0.01, 0.01, 0.01, 0.01, 0.01, 0.01)$, we apply the predictor-corrector method [40] to solve the fractional-order differential equations (10). The two- and three- dimensional phase planes of the nonautonomous fractional cardiac conduction system are shown in Figs. 3–4, which demonstrate the existence of hyperchaotic attractors in the fractional sense.

2.2.1 Equilibrium point and stability

The equilibrium point of the fractional model (10) and the associated Jacobian matrix, which have been given in Eqs. (5) and (8), respectively, are the same as model (2). The following lemma is also taken into account for investigating the stability of fractional-order mathematical systems.

Lemma 2.1 ([41]) *The equilibrium point of system* (10) *is locally asymptotically stable if all eigenvalues of the Jacobian matrix related to the equilibrium point E meet the following inequality*:

$$
\left|\arg(\lambda_i)\right| > \frac{\pi}{2}q, q = \max\{q_1, q_2, q_3, q_4, q_5, q_6\}.
\tag{11}
$$

3 Hyperchaos control and synchronization

This section considers the nonautonomous cardiac conduction system in both forms of integer- and fractional-order models (2) and (10), respectively. In this section, first we design optimal controllers in order to overcome the hyperchaotic oscillators with regard to the PMP [42–44]. Moreover, using the stability Lyapunov theory, we introduce an adaptive controller to synchronize two similar integer-order oscillators. Then the fractional-order model (10) is considered, and an active controller is proposed for the purpose of synchronization in the fractional sense.

Figure 3 Two-dimensional phase planes of the fractional cardiac conduction model (10) for $q_i = 0.9$
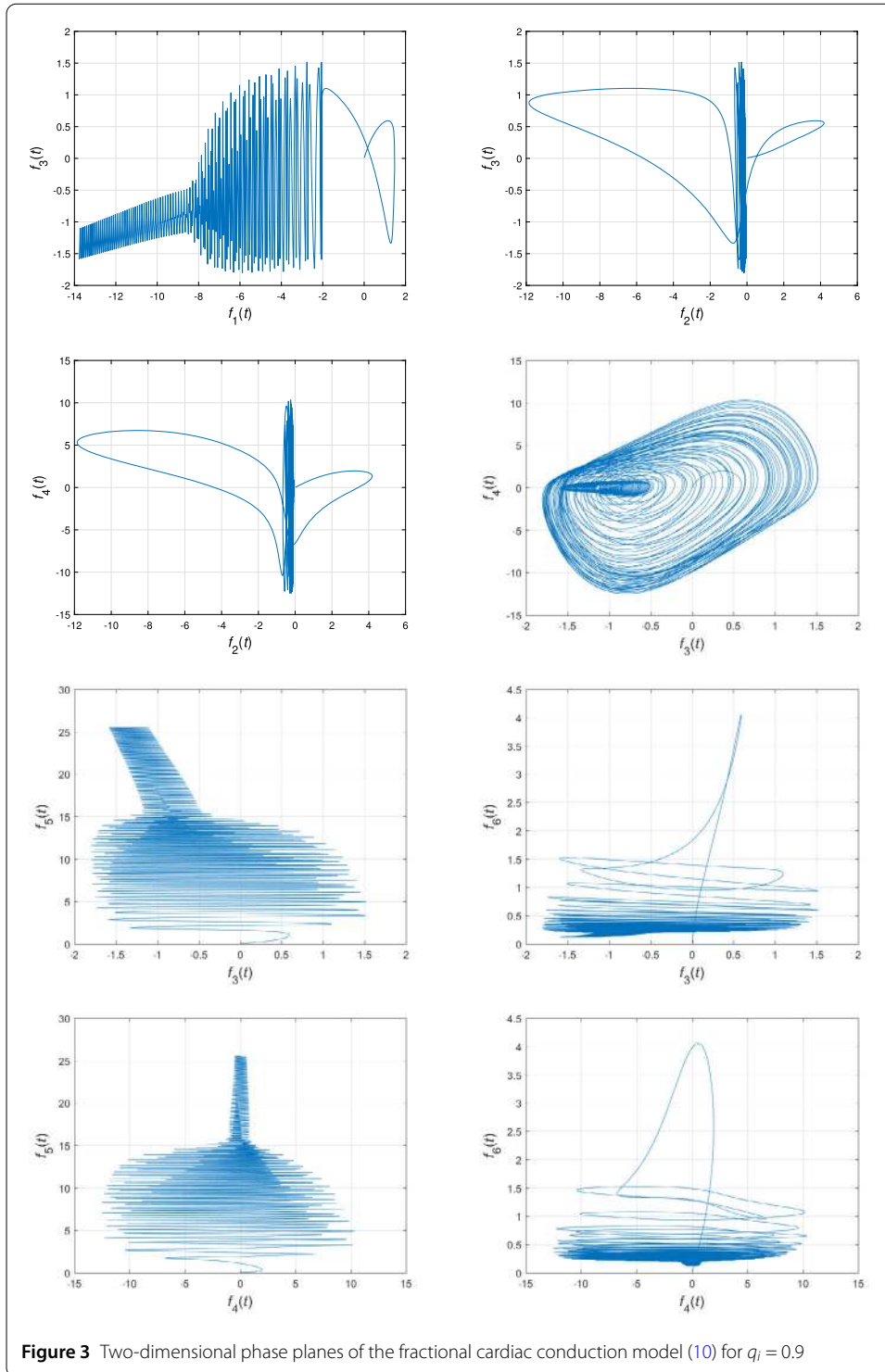
3.1 Optimal control

In this section, we stabilize the hyperchaotic behaviors of the integer-order nonautonomous system (2) as well as its fractional-order form by using optimal controllers based on the PMP.

Figure 4 Three-dimensional phase planes of the fractional cardiac conduction model (10) for $q_i = 0.9$
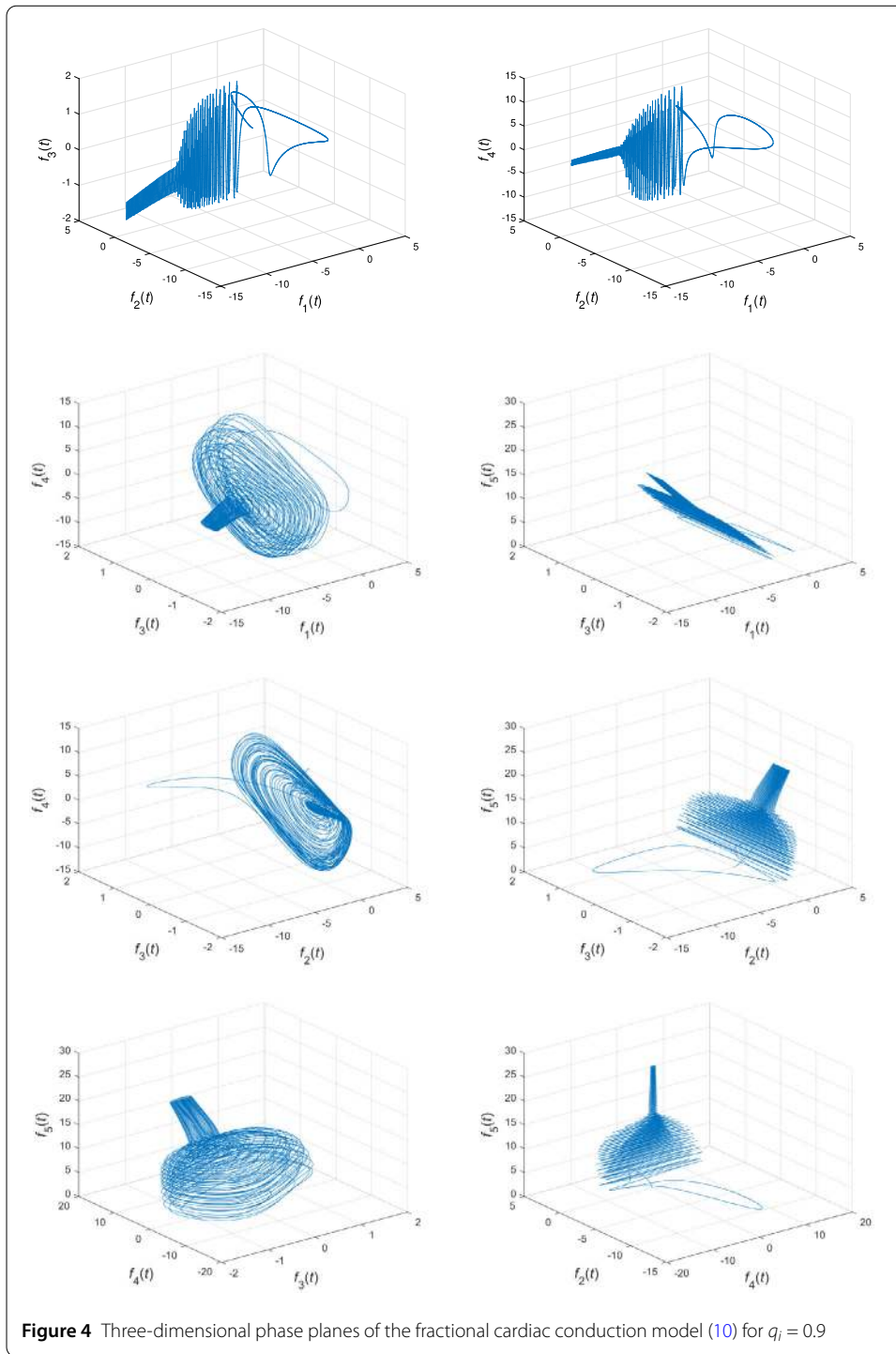
3.1.1 Integer-order case

As previously mentioned, this section aims at optimally controlling the nonlinear cardiac conduction system (2) using the PMP. To this aim, model (2) is rewritten in the following

form:

$$
\begin{cases}
\dot{f}_1 = f_2 + u_1, \\
\dot{f}_2 = -\alpha_1(f_1^2 - 1)f_2 - \beta_1 f_1 + \gamma_1 \cos(\omega t) + r_{13}(f_1 - f_3) + r_{15}(f_1 - f_5) + u_2, \\
\dot{f}_3 = f_4 + u_3, \\
\dot{f}_4 = -\alpha_2(f_3^2 - 1)f_4 - \beta_2 f_3 + \gamma_2 \cos(\omega t) + r_{31}(f_3 - f_1) + r_{35}(f_3 - f_5) + u_4, \\
\dot{f}_5 = f_6 + u_5, \\
\dot{f}_6 = -\alpha_3(f_5^2 - 1)f_6 - \beta_3 f_5 + \gamma_3 \cos(\omega t) + r_{51}(f_5 - f_1) + r_{53}(f_5 - f_3) + u_6,
\end{cases}
\tag{12}
$$

in which u_i is the control input. In addition, the performance index is defined by

$$
J = \frac{1}{2} \int_0^{t_f} \sum_{i=1}^{6} \left(v_i \big(f_i(t) - e_i(t)\big)^2 + w_i u_i^2(t) \right) dt,
\tag{13}
$$

where $v_i \geq 0$ and $w_i > 0$ are weighting coefficients, $e_i(t)$ is the ith coordinate of the equilibrium E, and t_f is the final time. Note that v_i is chosen in a way that the state variables are likely to converge on E for all $t \in (0, t_f)$. Furthermore, w_i is chosen so that the control input does not violate its bounds. The boundary conditions for the states are also considered by
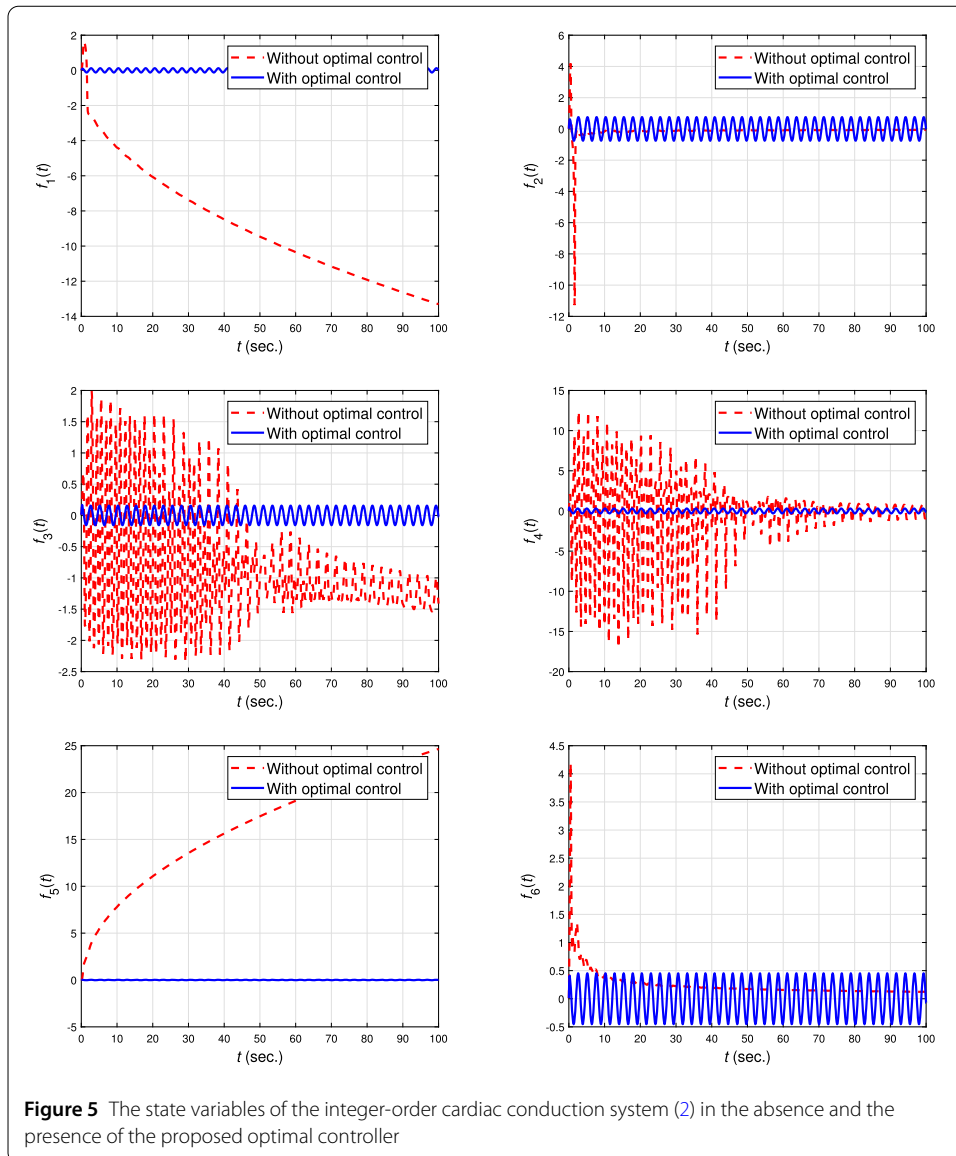
$$
f(0) = f_0, \qquad f(t_f) = E,
\tag{14}
$$

where $f(0)$ is an arbitrary initial vector, $f(t) = (f_1(t), f_2(t), f_3(t), f_4(t), f_5(t), f_6(t))$, and E is the unique equilibrium point. The necessary conditions of optimality for the optimal control problem (12)–(14) are obtained by

$$
\begin{cases}
\dot{f}_1 = f_2 - \frac{1}{w_1} g_1, \\
\dot{f}_2 = -\alpha_1(f_1^2 - 1)f_2 - \beta_1 f_1 + \gamma_1 \cos(\omega t) + r_{13}(f_1 - f_3) + r_{15}(f_1 - f_5) - \frac{1}{w_2} g_2, \\
\dot{f}_3 = f_4 - \frac{1}{w_3} g_3, \\
\dot{f}_4 = -\alpha_2(f_3^2 - 1)f_4 - \beta_2 f_3 + \gamma_2 \cos(\omega t) + r_{31}(f_3 - f_1) + r_{35}(f_3 - f_5) - \frac{1}{w_4} g_4, \\
\dot{f}_5 = f_6 - \frac{1}{w_5} g_5, \\
\dot{f}_6 = -\alpha_3(f_5^2 - 1)f_6 - \beta_3 f_5 + \gamma_3 \cos(\omega t) + r_{51}(f_5 - f_1) + r_{53}(f_5 - f_3) - \frac{1}{w_6} g_6,
\end{cases}
\tag{15}
$$

$$
\begin{cases}
\dot{g}_1 = v_1 e_1 - v_1 f_1 - (2\alpha_1 f_1 f_2 - \beta_1 + r_{13} + r_{15}) g_2 - (-r_{31}) g_4 - (-r_{51}) g_6, \\
\dot{g}_2 = v_2 e_2 - v_2 f_2 - g_1 + \alpha_1(f_1^2 - 1) g_2, \\
\dot{g}_3 = v_3 e_3 - v_3 f_3 + r_{31} g_2 + (2\alpha_2 f_3 f_4 + \beta_2 - r_{31} - r_{35}) g_4 + (\beta_3 + r_{53}) g_6, \\
\dot{g}_4 = v_4 e_4 - v_4 f_4 - g_3 + \alpha_2(f_3^2 - 1) g_4, \\
\dot{g}_5 = v_5 e_5 - v_5 f_5 + r_{15} g_2 + r_{35} g_4 + 2\alpha_3 f_5 f_6 g_6 + \beta_3 g_6 - r_{51} g_6 - r_{53} g_6, \\
\dot{g}_6 = v_6 e_6 - v_6 f_6 - g_5 + \alpha_3(f_5^2 - 1) g_6,
\end{cases}
\tag{16}
$$

where g_i denotes the co-state variable. As can be seen, a nonlinear two-point boundary value problem (BVP) is formed by the necessary conditions of optimality (15)–(16) and

Figure 5 The state variables of the integer-order cardiac conduction system (2) in the absence and the presence of the proposed optimal controller

the boundary conditions (14). Also, the optimal control is computed by

$$
u^*(t) = \begin{bmatrix} u_1^* \\ u_2^* \\ u_3^* \\ u_4^* \\ u_5^* \\ u_6^* \end{bmatrix} = - \begin{bmatrix} \frac{1}{w_1} g_1(t) \\ \frac{1}{w_2} g_2(t) \\ \frac{1}{w_3} g_3(t) \\ \frac{1}{w_4} g_4(t) \\ \frac{1}{w_5} g_5(t) \\ \frac{1}{w_6} g_6(t) \end{bmatrix}, \quad 0 \le t \le t_f.
\tag{17}
$$

Considering $t_f = 5$, $w_i = v_i = 1$, the parameter values as in Table 1, and the initial conditions $f_0 = (0.01, 0.01, 0.01, 0.01, 0.01, 0.01)$, we solve the aforesaid BVP numerically [45, 46]. In Fig. 5, the state trajectories of the considered system in the absence and the presence of control are compared. It is obvious that the state variables converge and stay near the origin.

3.1.2 Fractional-order case

In this section, we propose an optimal chaos controller in order to diminish the hyperchaotic behaviors of the nonautonomous cardiac conduction system modeled by the fractional-order dynamical equations (10). To do so, consider the controlled fractional-order model as follows:

$$
\begin{cases}
{}^{C}_{0}\mathscr{D}^{q_1}_t f_1 = f_2 + u_1, \\
{}^{C}_{0}\mathscr{D}^{q_2}_t f_2 = -\alpha_1(f_1^2 - 1)f_2 - \beta_1 f_1 + \gamma_1 \cos(\omega t) \\
\qquad\qquad + r_{13}(f_1 - f_3) + r_{15}(f_1 - f_5) + u_2, \\
{}^{C}_{0}\mathscr{D}^{q_3}_t f_3 = f_4 + u_3, \\
{}^{C}_{0}\mathscr{D}^{q_4}_t f_4 = -\alpha_2(f_3^2 - 1)f_4 - \beta_2 f_3 + \gamma_2 \cos(\omega t) + r_{31}(f_3 - f_1) \\
\qquad\qquad + r_{35}(f_3 - f_5) + u_4, \\
{}^{C}_{0}\mathscr{D}^{q_5}_t f_5 = f_6 + u_5, \\
{}^{C}_{0}\mathscr{D}^{q_6}_t f_6 = -\alpha_3(f_5^2 - 1)f_6 - \beta_3 f_5 + \gamma_3 \cos(\omega t) + r_{51}(f_5 - f_1) \\
\qquad\qquad + r_{53}(f_5 - f_3) + u_6.
\end{cases}
\tag{18}
$$

The purpose is to obtain the optimal control $u^*(t)$ along with minimizing the objective functional (13). In order to solve the above-mentioned fractional optimal control problem, we should derive the associated necessary optimality conditions. For this purpose, considering the fractional optimal control theory, we have the following scaler Hamiltonian function:

$$
H(t) = M_0(t) + \sum_{1}^{6} g_i(t) M_i(t),
\tag{19}
$$

where M_0 is the integrand function in (13), M_i is the right-hand side of the ith equation in (18), and g_i is the Lagrange multiplier also known as the costate variable. Following [47–49], the necessary optimality conditions of the aforesaid problem are obtained as follows:

$$
\begin{cases}
{}^{C}_{0}\mathscr{D}^{q_1}_t f_1 = \frac{\partial H}{\partial g_1}(t) = f_2 + u_1^*, \\
{}^{C}_{0}\mathscr{D}^{q_2}_t f_2 = \frac{\partial H}{\partial g_2}(t) = -\alpha_1(f_1^2 - 1)f_2 - \beta_1 f_1 + \gamma_1 \cos(\omega t) \\
\qquad\qquad + r_{13}(f_1 - f_3) + r_15(f_1 - f_5) + u_2^*, \\
{}^{C}_{0}\mathscr{D}^{q_3}_t f_3 = \frac{\partial H}{\partial g_3}(t) = f_4 + u_3^*, \\
{}^{C}_{0}\mathscr{D}^{q_4}_t f_4 = \frac{\partial H}{\partial g_4}(t) = -\alpha_2(f_3^2 - 1)f_4 - \beta_2 f_3 + \gamma_2 \cos(\omega t) \\
\qquad\qquad + r_{31}(f_3 - f_1) + r_35(f_3 - f_5) + u_4^*, \\
{}^{C}_{0}\mathscr{D}^{q_5}_t f_5 = \frac{\partial H}{\partial g_5}(t) = f_6 + u_5^*, \\
{}^{C}_{0}\mathscr{D}^{q_6}_t f_6 = \frac{\partial H}{\partial g_6}(t) = -\alpha_3(f_5^2 - 1)f_6 - \beta_3 f_5 + \gamma_3 \cos(\omega t) \\
\qquad\qquad + r_{51}(f_5 - f_1) + r_53(f_5 - f_3) + u_6^*,
\end{cases}
\tag{20}
$$

$$
\begin{cases}
{}_t^C\mathscr{D}_{t_f}^{q_1} g_1 = \frac{\partial H}{\partial f_1}(t) = \nu_1 f_1 - \nu_1 e_1 + (2\alpha_1 f_1 f_2 - \beta_1 + r_{13} + r_{15})g_2 \\
\qquad\qquad\qquad + (-r_{31})g_4 + (-r_{51})g_6, \\
{}_t^C\mathscr{D}_{t_f}^{q_2} g_2 = \frac{\partial H}{\partial f_2}(t) = \nu_2 f_2 - \nu_2 e_2 + g_1 - \alpha_1(f_1^2 - 1)g_2, \\
{}_t^C\mathscr{D}_{t_f}^{q_3} g_3 = \frac{\partial H}{\partial f_3}(t) = \nu_3 f_3 - \nu_3 e_3 - r_{31}g_2 - (2\alpha_2 f_3 f_4 + \beta_2 - r_{31} - r_{35})g_4 \\
\qquad\qquad\qquad - (\beta_3 + r_{53})g_6, \\
{}_t^C\mathscr{D}_{t_f}^{q_4} g_4 = \frac{\partial H}{\partial f_4}(t) = \nu_4 f_4 - \nu_4 e_4 + g_3 - \alpha_2(f_3^2 - 1)g_4, \\
{}_t^C\mathscr{D}_{t_f}^{q_5} g_5 = \frac{\partial H}{\partial f_5}(t) = \nu_5 f_5 - \nu_5 e_5 - r_{15}g_2 - r_{35}g_4 - 2\alpha_3 f_5 f_6 g_6 \\
\qquad\qquad\qquad - \beta_3 g_6 + r_{51}g_6 + r_{53}g_6, \\
{}_t^C\mathscr{D}_{t_f}^{q_6} g_6 = \frac{\partial H}{\partial f_6}(t) = \nu_6 f_6 - \nu_6 e_6 + g_5 - \alpha_3(f_5^2 - 1)g_6.
\end{cases}
\tag{21}
$$

$$
\begin{cases}
\frac{\partial H}{\partial u_1}(t) = w_1 u_1(t) + g_1(t) = 0 \Rightarrow u_1^*(t) = -\frac{1}{w_1}g_1(t), \\
\frac{\partial H}{\partial u_2}(t) = w_2 u_2(t) + g_2(t) = 0 \Rightarrow u_2^*(t) = -\frac{1}{w_2}g_2(t), \\
\frac{\partial H}{\partial u_3}(t) = w_1 u_3(t) + g_3(t) = 0 \Rightarrow u_3^*(t) = -\frac{1}{w_3}g_3(t), \\
\frac{\partial H}{\partial u_4}(t) = w_2 u_4(t) + g_4(t) = 0 \Rightarrow u_4^*(t) = -\frac{1}{w_4}g_4(t), \\
\frac{\partial H}{\partial u_5}(t) = w_1 u_5(t) + g_5(t) = 0 \Rightarrow u_5^*(t) = -\frac{1}{w_5}g_5(t), \\
\frac{\partial H}{\partial u_6}(t) = w_2 u_6(t) + g_6(t) = 0 \Rightarrow u_6^*(t) = -\frac{1}{w_6}g_6(t),
\end{cases}
\tag{22}
$$

together with the initial values $f(0) = f_0$ and the transversality conditions $g_i(t_f) = 0$, $i = 1,\ldots 6$, where ${}_t^C\mathscr{D}_{t_f}^{q_i}$ denotes the right Caputo fractional derivative. In order to solve Eqs. (20) and (21), we utilize the proposed numerical approach in [47], which is a combination of a developed predictor-corrector method and a forward-backward sweep iterative algorithm. Simulation results in Fig. 6 illustrate that the hyperchaotic behaviors of the fractional-order cardiac conduction system (10) are controlled via the presented fractional-order optimal controller, so the controlled fractional system reveals stable periodic solutions.
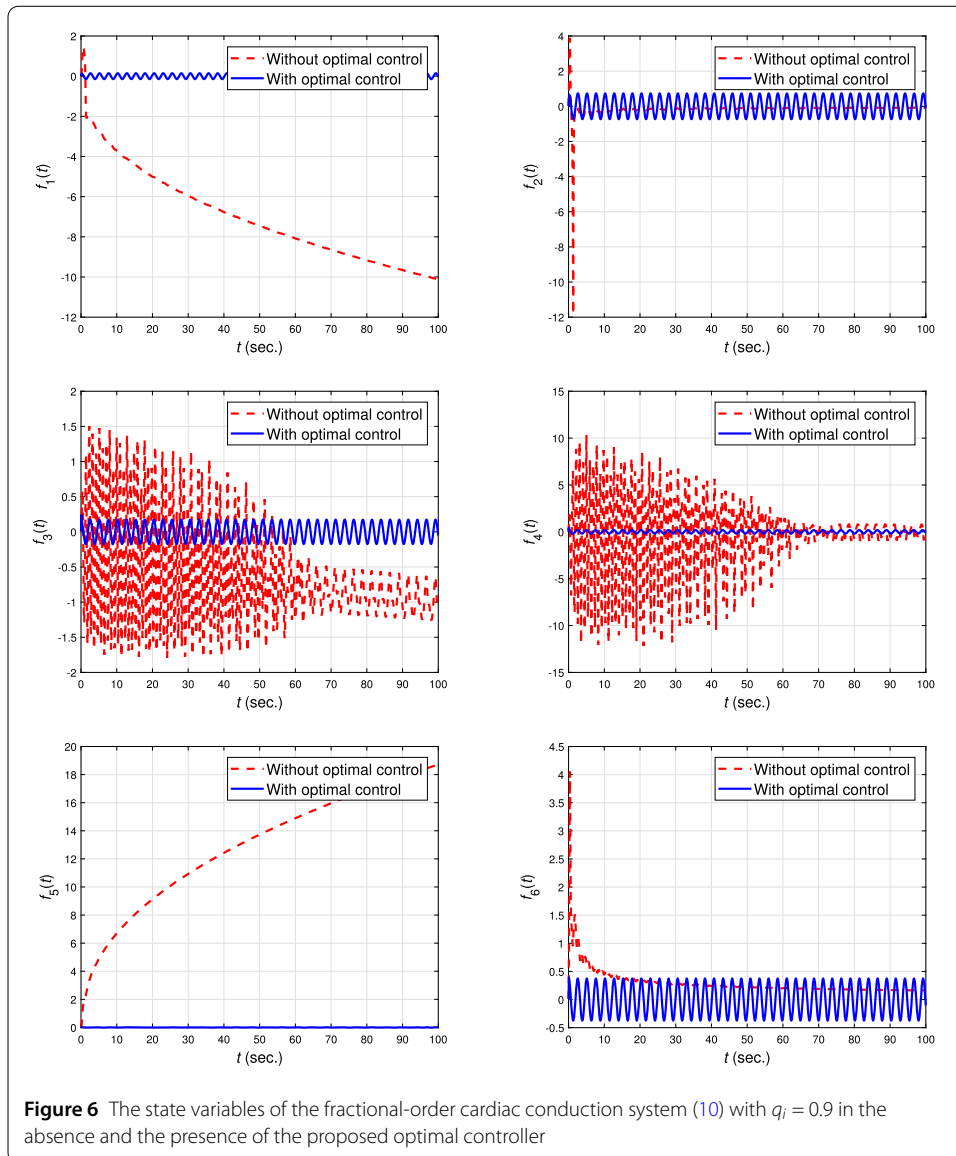
3.2 Synchronization

In this section, we synchronize two identical hyperchaotic conduction systems in the frameworks of classical and fractional calculus by applying an adaptive and an active controller, respectively.

3.2.1 Integer-order case

Nonlinear nonautonomous biological systems are generally hard to synchronize due to the complexity of their hyperchaotic behaviors. Thus, we apply a systematic synchronization action plan to reach the synchronization purpose in this section. To this aim, we consider Eq. (2) as the master system, while the slave system is taken from

$$
\begin{cases}
\dot{g}_1 = g_2 + u_1, \\
\dot{g}_2 = -\alpha_1(g_1^2 - 1)g_2 - \beta_1 g_1 + \gamma_1\cos(\omega t) + r_{13}(g_1 - g_3) + r_{15}(g_1 - g_5) + u_2, \\
\dot{g}_3 = g_4 + u_3, \\
\dot{g}_4 = -\alpha_2(g_3^2 - 1)g_4 - \beta_2 g_3 + \gamma_2\cos(\omega t) + r_{31}(g_3 - g_1) + r_{35}(g_3 - g_5) + u_4, \\
\dot{g}_5 = g_6 + u_5, \\
\dot{g}_6 = -\alpha_3(g_5^2 - 1)g_6 - \beta_3 g_5 + \gamma_3\cos(\omega t) + r_{51}(g_5 - g_1) + r_{53}(g_5 - g_3) + u_6,
\end{cases}
\tag{23}
$$

Figure 6 The state variables of the fractional-order cardiac conduction system (10) with $q_i = 0.9$ in the absence and the presence of the proposed optimal controller

in which u_i and g_i are the control input and the state variable of the slave model, respectively. Assuming $e_i(t) = g_i(t) - f_i(t)$ as the error of synchronization, we derive the error dynamical equations as

$$
\begin{cases}
\dot{e}_1 = e_2 + u_1, \\
\dot{e}_2 = -\alpha_1(g_1^2 g_2 - f_1^2 f_2 - e_2) - \beta_1 e_1 + r_{13}(e_1 - e_3) + r_{15}(e_1 - e_5) + u_2, \\
\dot{e}_3 = e_4 + u_3, \\
\dot{e}_4 = -\alpha_2(g_3^2 g_4 - f_3^2 f_4 - e_4) - \beta_2 e_3 + r_{31}(e_3 - e_1) + r_{35}(e_3 - e_5) + u_4, \\
\dot{e}_5 = e_6 + u_5, \\
\dot{e}_6 = -\alpha_3(g_5^2 g_6 - f_5^2 f_6 - e_6) - \beta_3 e_5 + r_{51}(e_5 - e_1) + r_{53}(e_5 - e_3) + u_6.
\end{cases}
\tag{24}
$$

Theorem 3.1 *The nonautonomous hyperchaotic conduction systems* (2) *and* (24) *can be globally and asymptotically synchronized by using the following adaptive control law*:

$$
\begin{cases}
u_1 = -e_2 - b_1 e_1, \\
u_2 = \hat{\alpha}_1 (g_1^2 g_2 - f_1^2 f_2 - e_2) + \hat{\beta}_1 e_1 - \hat{r}_{13}(e_1 - e_3) \\
\qquad - \hat{r}_{15}(e_1 - e_5) - b_2 e_2, \\
u_3 = -e_4 - b_3 e_3, \\
u_4 = \hat{\alpha}_2 (g_3^2 g_4 - f_3^2 f_4 - e_4) + \hat{\beta}_2 e_3 - \hat{r}_{31}(e_3 - e_1) \\
\qquad - \hat{r}_{35}(e_3 - e_5) - b_4 e_4, \\
u_5 = -e_6 - b_5 e_5, \\
u_6 = \hat{\alpha}_3 (g_5^2 g_6 - f_5^2 f_6 - e_6) + \hat{\beta}_3 e_5 - \hat{r}_{51}(e_5 - e_1) \\
\qquad - \hat{r}_{53}(e_5 - e_3) - b_6 e_6,
\end{cases}
\tag{25}
$$

together with the following parameter updating law:

$$
\begin{cases}
\dot{\hat{\alpha}}_1 = e_2(e_2 + f_1^2 f_2 - g_1^2 g_2), \\
\dot{\hat{\alpha}}_2 = e_4(e_4 + f_3^2 f_4 - g_3^2 g_4), \\
\dot{\hat{\alpha}}_3 = e_6(e_6 + f_5^2 f_6 - g_5^2 g_6), \\
\dot{\hat{\beta}}_1 = -e_1 e_2, \\
\dot{\hat{\beta}}_2 = -e_3 e_4, \\
\dot{\hat{\beta}}_3 = -e_5 e_6, \\
\dot{\hat{\gamma}}_1 = 0, \\
\dot{\hat{\gamma}}_2 = 0, \\
\dot{\hat{\gamma}}_3 = 0, \\
\dot{\hat{r}}_{13} = e_1 e_2 - e_2 e_3, \\
\dot{\hat{r}}_{15} = e_1 e_2 - e_2 e_5, \\
\dot{\hat{r}}_{31} = e_3 e_4 - e_4 e_1, \\
\dot{\hat{r}}_{35} = e_3 e_4 - e_4 e_5, \\
\dot{\hat{r}}_{51} = e_5 e_6 - e_6 e_1, \\
\dot{\hat{r}}_{53} = e_5 e_6 - e_6 e_3,
\end{cases}
\tag{26}
$$

in which the uncertain parameters $\alpha_1, \alpha_2, \alpha_3, \beta_1, \beta_2, \beta_3, \gamma_1, \gamma_2, \gamma_3, r_{13}, r_{15}, r_{31}, r_{35}, r_{51}, r_{53}$ *are estimated by* $\hat{\alpha}_1, \hat{\alpha}_2, \hat{\alpha}_3, \hat{\beta}_1, \hat{\beta}_2, \hat{\beta}_3, \hat{\gamma}_1, \hat{\gamma}_2, \hat{\gamma}_3, \hat{r}_{13}, \hat{r}_{15}, \hat{r}_{31}, \hat{r}_{35}, \hat{r}_{51}, \hat{r}_{53}$, *respectively, and* $b_i \geq 0$ *is a constant gain.*

Proof Substituting (25) into (24), we have

$$
\begin{cases}
\dot{e}_1 = -b_1 e_1, \\
\dot{e}_2 = -(\alpha_1 - \hat{\alpha}_1)(g_1^2 g_2 - f_1^2 f_2 - e_2) - (\beta_1 - \hat{\beta}_1)e_1 + (r_{13} - \hat{r}_{13})(e_1 - e_3) \\
\qquad + (r_{15} - \hat{r}_{15})(e_1 - e_5) - b_2 e_2, \\
\dot{e}_3 = -b_3 e_3, \\
\dot{e}_4 = -(\alpha_2 - \hat{\alpha}_2)(g_3^2 g_4 - f_3^2 f_4 - e_4) - (\beta_2 - \hat{\beta}_2)e_3 + (r_{31} - \hat{r}_{31})(e_3 - e_1) \\
\qquad + (r_{35} - \hat{r}_{35})(e_3 - e_5) - b_4 e_4, \\
\dot{e}_5 = -b_5 e_5, \\
\dot{e}_6 = -(\alpha_5 - \hat{\alpha}_5)(g_5^2 g_6 - f_5^2 f_6 - e_6) - (\beta_3 - \hat{\beta}_3)e_5 + (r_{51} - \hat{r}_{51})(e_5 - e_1) \\
\qquad + (r_{53} - \hat{r}_{53})(e_5 - e_3) - b_6 e_6,
\end{cases}
\tag{27}
$$

which can be rewritten as

$$
\begin{cases}
\dot{e}_1 = -b_1 e_1, \\
\dot{e}_2 = -\tilde{\alpha}_1(g_1^2 g_2 - f_1^2 f_2 - e_2) - \tilde{\beta}_1 e_1 + \tilde{r}_{13}(e_1 - e_3) + \tilde{r}_{15}(e_1 - e_5) - b_2 e_2, \\
\dot{e}_3 = -b_3 e_3, \\
\dot{e}_4 = -\tilde{\alpha}_2(g_3^2 g_4 - f_3^2 f_4 - e_4) - \tilde{\beta}_2 e_3 + \tilde{r}_{31}(e_3 - e_1) + \tilde{r}_{35}(e_3 - e_5) - b_4 e_4, \\
\dot{e}_5 = -b_5 e_5, \\
\dot{e}_6 = -\tilde{\alpha}_3(g_5^2 g_6 - f_5^2 f_6 - e_6) - \tilde{\beta}_3 e_5 + \tilde{r}_{51}(e_5 - e_1) + \tilde{r}_{53}(e_5 - e_3) - b_6 e_6,
\end{cases}
\tag{28}
$$

in which

$$
\begin{cases}
\tilde{\gamma}_1 = \gamma_1 - \hat{\gamma}_1, & \tilde{\gamma}_2 = \gamma_2 - \hat{\gamma}_2, & \tilde{\gamma}_3 = \gamma_3 - \hat{\gamma}_3, \\
\tilde{\alpha}_1 = \alpha_1 - \hat{\alpha}_1, & \tilde{\alpha}_2 = \alpha_2 - \hat{\alpha}_2, & \tilde{\alpha}_3 = \alpha_3 - \hat{\alpha}_3, \\
\tilde{\beta}_1 = \beta_1 - \hat{\beta}_1, & \tilde{\beta}_2 = \beta_2 - \hat{\beta}_2, & \tilde{\beta}_3 = \beta_3 - \hat{\beta}_3, \\
\tilde{r}_{13} = r_{13} - \hat{r}_{13}, & \tilde{r}_{15} = r_{15} - \hat{r}_{15}, \\
\tilde{r}_{31} = r_{31} - \hat{r}_{31}, & \tilde{r}_{35} = r_{35} - \hat{r}_{35}, \\
\tilde{r}_{51} = r_{51} - \hat{r}_{51}, & \tilde{r}_{53} = r_{53} - \hat{r}_{53}.
\end{cases}
\tag{29}
$$

Also, the related derivatives are stated by

$$
\begin{cases}
\dot{\tilde{\gamma}}_1 = -\dot{\hat{\gamma}}_1, & \dot{\tilde{\gamma}}_2 = -\dot{\hat{\gamma}}_2, & \dot{\tilde{\gamma}}_3 = -\dot{\hat{\gamma}}_3, \\
\dot{\tilde{\alpha}}_1 = -\dot{\hat{\alpha}}_1, & \dot{\tilde{\alpha}}_2 = -\dot{\hat{\alpha}}_2, & \dot{\tilde{\alpha}}_3 = -\dot{\hat{\alpha}}_3, \\
\dot{\tilde{\beta}}_1 = -\dot{\hat{\beta}}_1, & \dot{\tilde{\beta}}_2 = -\dot{\hat{\beta}}_2, & \dot{\tilde{\beta}}_3 = -\dot{\hat{\beta}}_3, \\
\dot{\tilde{r}}_{13} = -\dot{\hat{r}}_{13}, & \dot{\tilde{r}}_{15} = -\dot{\hat{r}}_{15}, \\
\dot{\tilde{r}}_{31} = -\dot{\hat{r}}_{31}, & \dot{\tilde{r}}_{35} = -\dot{\hat{r}}_{35}, \\
\dot{\tilde{r}}_{51} = -\dot{\hat{r}}_{51}, & \dot{\tilde{r}}_{53} = -\dot{\hat{r}}_{53}.
\end{cases}
\tag{30}
$$

Then we suppose the following Lyapunov function and its derivative for the model stated in Eqs. (28) and (30):

$$V = \frac{1}{2}\left(\Sigma_{i=1}^{6}e_i^2 + \Sigma_{i=1}^{3}(\tilde{\alpha}_i^2 + \tilde{\beta}_i^2 + \tilde{\gamma}_i^2) + \tilde{r}_{13}^2 + \tilde{r}_{15}^2 + \tilde{r}_{31}^2 + \tilde{r}_{35}^2 + \tilde{r}_{51}^2 + \tilde{r}_{53}^2\right), \tag{31}$$

$$\begin{aligned}
\dot{V} = &-\Sigma_{i=1}^{6}b_i e_i^2 - \Sigma_{i=1}^{3}\tilde{\gamma}_i\dot{\tilde{\gamma}}_i - \tilde{\beta}_1(e_1 e_2 + \dot{\tilde{\beta}}_1) \\
&- \tilde{\beta}_2(e_3 e_4 + \dot{\tilde{\beta}}_2) - \tilde{\beta}_3(e_5 e_6 + \dot{\tilde{\beta}}_3) - \tilde{\alpha}_1(\dot{\tilde{\alpha}}_1 + e_2 g_1^2 g_2 - e_2 f_1^2 f_2 - e_2^2) \\
&- \tilde{\alpha}_2(\dot{\tilde{\alpha}}_2 + e_4 g_3^2 g_4 - e_4 f_3^2 f_4 - e_4^2) - \tilde{\alpha}_3(\dot{\tilde{\alpha}}_3 + e_6 g_5^2 g_6 - e_6 f_5^2 f_6 - e_6^2) \\
&- \tilde{r}_{13}(\dot{\tilde{r}}_{13} - e_1 e_2 + e_2 e_3) - \tilde{r}_{15}(\dot{\tilde{r}}_{15} - e_1 e_2 + e_2 e_5) - \tilde{r}_{31}(\dot{\tilde{r}}_{31} - e_3 e_4 + e_1 e_4) \\
&- \tilde{r}_{35}(\dot{\tilde{r}}_{35} - e_3 e_4 + e_4 e_5) - \tilde{r}_{51}(\dot{\tilde{r}}_{51} - e_5 e_6 + e_1 e_6) - \tilde{r}_{53}(\dot{\tilde{r}}_{53} - e_5 e_6 + e_3 e_6),
\end{aligned} \tag{32}$$

respectively. Applying the parameter update law from Eq. (26), we get

$$\dot{V} = -\Sigma_{i=1}^{6}b_i e_i^2. $$

If we consider $b = \min\{b_1, b_2, b_3, b_4, b_5, b_6\}$, then $\dot{V} \leq -b\|e(t)\|_2^2$. Integrating both sides of this inequality, we have
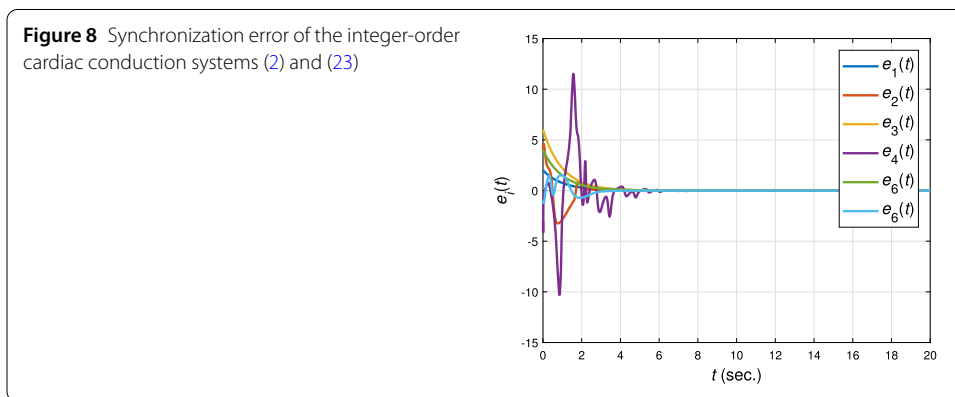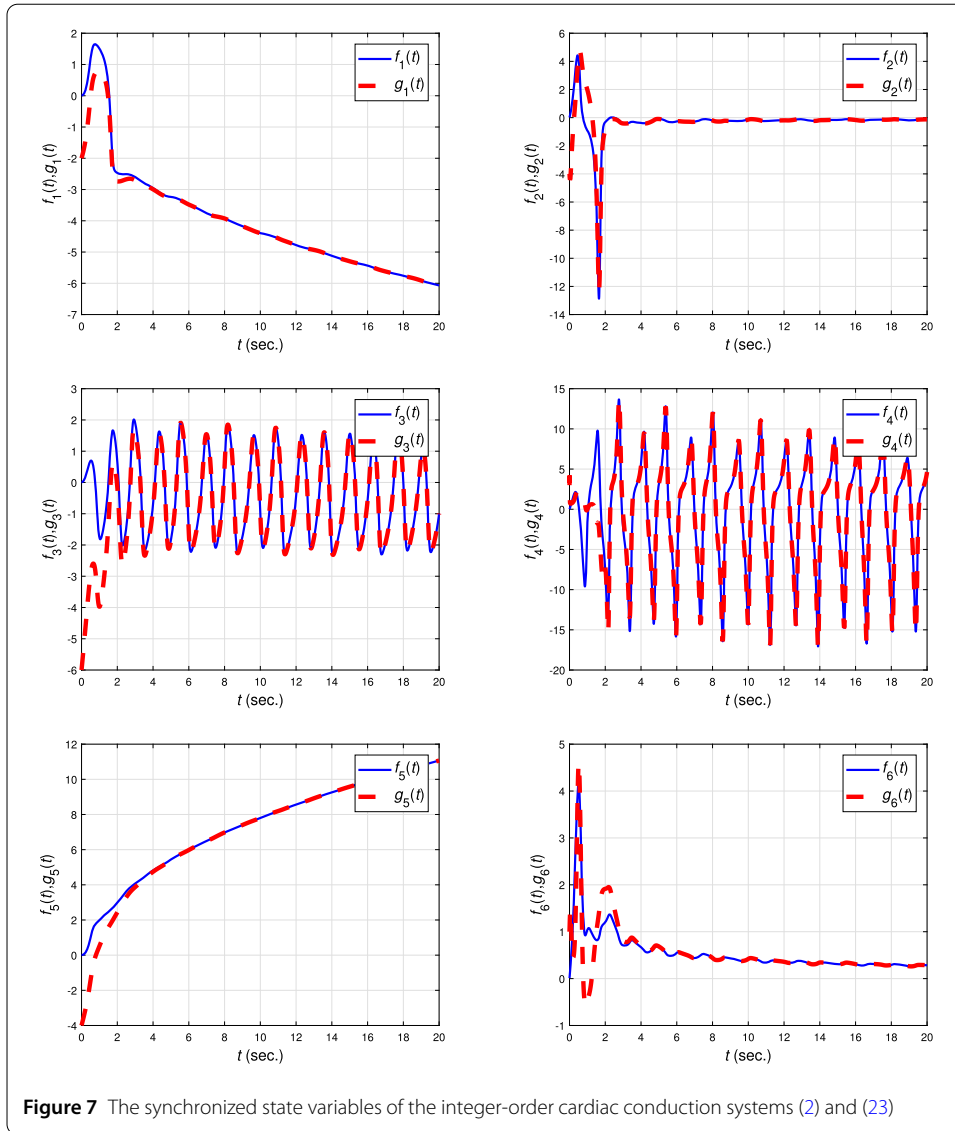
$$\int_0^t \|e(\tau)\|_2^2 \, d\tau \leq \frac{V(0) - V(t)}{b} < \infty. \tag{33}$$

Applying Barbalat's lemma [37], considering the fact that $\dot{e}(t) \in L_\infty$ and $e(t) \in L_2$ (concluded from Eqs. (28) and (33)), and using the proposed control input (25), we can conclude that the considered hyperchaotic conduction systems (2) and (24) are synchronized asymptotically and globally, the fact which reveals that the error of synchronization converges to the origin in an asymptotic manner. □

To illustrate the effective performance of Theorem 3.1, we take into account the initial states and parameters as follows:

$$\begin{cases}
(f_1(0), f_2(0), f_3(0), f_4(0), f_5(0), f_6(0)) = (0.01, 0.01, 0.01, 0.01, 0.01, 0.01), \\
(g_1(0), g_2(0), g_3(0), g_4(0), g_5(0), g_6(0)) = (-2, -4, -6, 3, -4, 1), \\
(\hat{\alpha}_1(0), \hat{\alpha}_2(0), \hat{\alpha}_3(0), \hat{\beta}_1(0), \hat{\beta}_2(0), \hat{\beta}_3(0)) = (7, 8, 6, 2, 5, 1), \\
(\hat{\gamma}_1(0), \hat{\gamma}_2(0), \hat{\gamma}_3(0)) = (5, 6, 4), \\
(\hat{r}_{13}(0), \hat{r}_{15}(0), \hat{r}_{31}(0), \hat{r}_{35}(0), \hat{r}_{51}(0), \hat{r}_{53}(0)) = (7, 2, 2, 3, 4, 7).
\end{cases} \tag{34}$$

Additionally, the constant gains are set to be $b_1 = b_2 = b_3 = b_4 = b_5 = b_6 = 1$. The synchronized state trajectories as well as the synchronization errors are depicted in Figs. 7 and 8, respectively.

Figure 7 The synchronized state variables of the integer-order cardiac conduction systems (2) and (23)

Figure 8 Synchronization error of the integer-order cardiac conduction systems (2) and (23)

3.2.2 Fractional-order case

In this section, in order to synchronize two identical fractional-order cardiac conduction systems, we design an efficient active control strategy. To this aim, we consider the

fractional-order model (10) as the master system and consider the slave one as follows:

$$
\begin{cases}
{}^{C}_{0}\mathscr{D}^{q_1}_t g_1 = g_2 + u_1, \\
{}^{C}_{0}\mathscr{D}^{q_2}_t g_2 = -\alpha_1(g_1^2 - 1)g_2 - \beta_1 g_1 + \gamma_1 \cos(\omega t) + r_{13}(g_1 - g_3) + r_{15}(g_1 - g_5) + u_2, \\
{}^{C}_{0}\mathscr{D}^{q_3}_t g_3 = g_4 + u_3, \\
{}^{C}_{0}\mathscr{D}^{q_4}_t g_4 = -\alpha_2(g_3^2 - 1)g_4 - \beta_2 g_3 + \gamma_2 \cos(\omega t) + r_{31}(g_3 - g_1) + r_{35}(g_3 - g_5) + u_4, \\
{}^{C}_{0}\mathscr{D}^{q_5}_t g_5 = g_6 + u_5, \\
{}^{C}_{0}\mathscr{D}^{q_6}_t g_6 = -\alpha_3(g_5^2 - 1)g_6 - \beta_3 g_5 + \gamma_3 \cos(\omega t) + r_{51}(g_5 - g_1) + r_{53}(g_5 - g_3) + u_6,
\end{cases}
\tag{35}
$$

where u_i and g_i are the control input and the state variable of the slave model, respectively. If we consider $e_i(t) = g_i(t) - f_i(t)$ as the synchronization error, then the dynamic of e_i is formulated by

$$
\begin{cases}
{}^{C}_{0}\mathscr{D}^{q_1}_t e_1 = e_2 + u_1, \\
{}^{C}_{0}\mathscr{D}^{q_2}_t e_2 = -\alpha_1(g_1^2 g_2 - f_1^2 f_2 - e_2) - \beta_1 e_1 + r_{13}(e_1 - e_3) + r_{15}(e_1 - e_5) + u_2, \\
{}^{C}_{0}\mathscr{D}^{q_3}_t e_3 = e_4 + u_3, \\
{}^{C}_{0}\mathscr{D}^{q_4}_t e_4 = -\alpha_2(g_3^2 g_4 - f_3^2 f_4 - e_4) - \beta_2 e_3 + r_{31}(e_3 - e_1) + r_{35}(e_3 - e_5) + u_4, \\
{}^{C}_{0}\mathscr{D}^{q_5}_t e_5 = e_6 + u_5, \\
{}^{C}_{0}\mathscr{D}^{q_6}_t e_6 = -\alpha_3(g_5^2 g_6 - f_5^2 f_6 - e_6) - \beta_3 e_5 + r_{51}(e_5 - e_1) + r_{53}(e_5 - e_3) + u_6.
\end{cases}
\tag{36}
$$

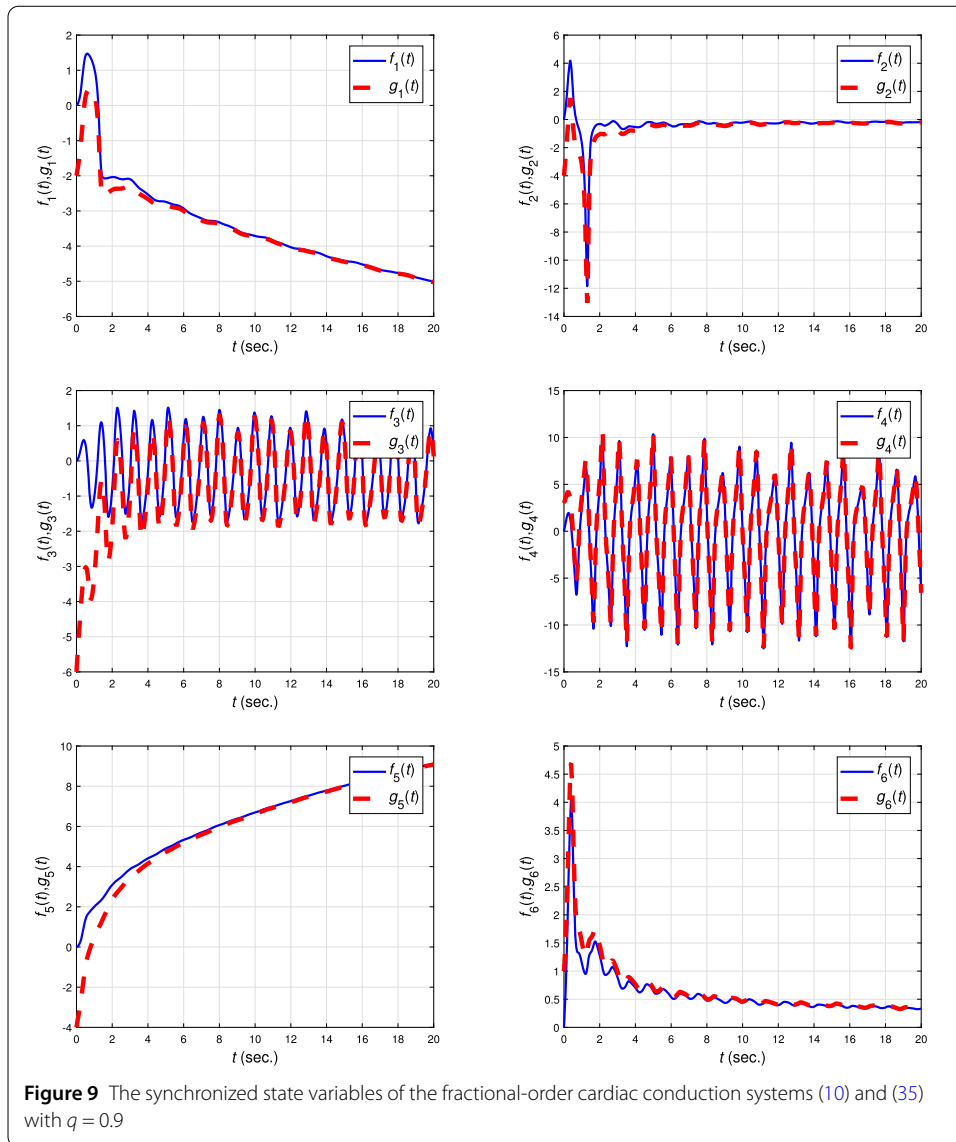Assume the control input as

$$
\begin{cases}
u_1 = r_1, \\
u_2 = r_2 + \alpha_1(g_1^2 g_2 - f_1^2 f_2), \\
u_3 = r_3, \\
u_4 = r_4 + \alpha_2(g_3^2 g_4 - f_3^2 f_4), \\
u_5 = r_5, \\
u_6 = r_6 + \alpha_3(g_5^2 g_6 - f_5^2 f_6),
\end{cases}
\tag{37}
$$

where $r_1, r_2, r_3, r_4, r_5, r_6$ are active control inputs. Substituting and rearranging (36) and (37), we derive the synchronization error dynamics in the form

$$
\begin{cases}
{}^{C}_{0}\mathscr{D}^{q_1}_t e_1 = e_2 + r_1, \\
{}^{C}_{0}\mathscr{D}^{q_2}_t e_2 = \alpha_1 e_2 - \beta_1 e_1 + r_{13}(e_1 - e_3) + r_{15}(e_1 - e_5) + r_2, \\
{}^{C}_{0}\mathscr{D}^{q_3}_t e_3 = e_4 + r_3, \\
{}^{C}_{0}\mathscr{D}^{q_4}_t e_4 = \alpha_2 e_4 - \beta_2 e_3 + r_{31}(e_3 - e_1) + r_{35}(e_3 - e_5) + r_4, \\
{}^{C}_{0}\mathscr{D}^{q_5}_t e_5 = e_6 + r_5, \\
{}^{C}_{0}\mathscr{D}^{q_6}_t e_6 = \alpha_3 e_6 - \beta_3 e_5 + r_{51}(e_5 - e_1) + r_{53}(e_5 - e_3) + r_6.
\end{cases}
\tag{38}
$$

Note that the active control inputs must be chosen such that the master and the slave systems are synchronized. Here, we suppose the following control inputs as an effective

Figure 9 The synchronized state variables of the fractional-order cardiac conduction systems (10) and (35) with $q = 0.9$
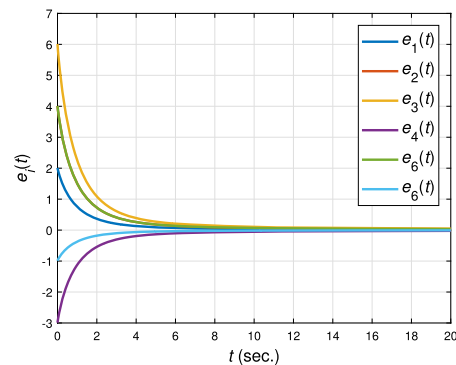
choice:

$$\begin{bmatrix} r_1 \\ r_2 \\ r_3 \\ r_4 \\ r_5 \\ r_6 \end{bmatrix} = A \begin{bmatrix} e_1 \\ e_2 \\ e_3 \\ e_4 \\ e_5 \\ e_6 \end{bmatrix}, \tag{39}$$

where

$$A = \begin{bmatrix} -1 & -1 & 0 & 0 & 0 & 0 \\ \beta_1 - r_{13} - r_{15} & -\alpha_1 - 1 & r_{13} & 0 & r_{15} & 0 \\ 0 & 0 & -1 & -1 & 0 & 0 \\ r_{31} & 0 & \beta_2 - r_{31} - r_{35} & -\alpha_2 - 1 & r_{35} & 0 \\ 0 & 0 & 0 & 0 & -1 & -1 \\ r_{51} & 0 & r_{53} & 0 & \beta_3 - r_{51} - r_{53} & -\alpha_3 - 1 \end{bmatrix}. \tag{40}$$

Figure 10 Synchronization error of the fractional-order cardiac conduction systems (10) and (35) with $q = 0.9$

Notice that there are other possibilities to choose the constant matrix A. The main point which should be taken into account is that the matrix A should be selected such that the conditions of stability in Lemma 2.1 are achieved. By considering the parameter values $(\alpha_1, \alpha_2, \alpha_3, \beta_1, \beta_2, \beta_3, \gamma_1, \gamma_2, \gamma_3, r_{13}, r_{15}, r_{31}, r_{35}, r_{51}, r_{53})$ as in Table 1, the initial values of the master and the slave systems as $f(0) = (0.01, 0.01, 0.01, 0.01, 0.01, 0.01)$ and $g(0) = (-2, -4, -6, 3, -4, 1)$, respectively, we simulate the results including the synchronized state trajectories and synchronization errors for $q_i = 0.9$ in Figs. 9–10, respectively.

4 Discussions and concluding remarks

In this paper, the hyperchaotic behaviors of a nonautonomous cardiac conduction system were investigated in both frames of integer- and fractional-order differential equations. Considering both cases, we designed optimal control strategies to stabilize the hyperchaotic state variables and diminish the hyperchaotic behaviors efficiently. These controllers were designed by applying the PMP for the necessary optimality conditions. Afterwards, we synchronized two similar conduction systems using an adaptive control scheme and an active controller, respectively, for the integer- and fractional-order models. More specifically, assuming parameter uncertainty, we synchronized two identical integer-order systems; the asymptotic stability of the synchronization error was proved by using Barbalat's lemma together with the stability theory of Lyapunov. Then considering the fractional-order mathematical model, we proposed an active controller to synchronize two identical fractional-order systems. As a result, the application of fractional calculus in this paper presented a more realistic and flexible performance to design well-organized control strategies for fractional-order models can describe memory effects which are the essential feature of many biological processes.

Availability of data and materials
Data sharing is not applicable to this article as no datasets were generated or analysed during the current study.

Competing interests
The authors declare that they have no competing interests.

Authors' contributions
The authors declare that the study was realized in collaboration with equal responsibility. All authors read and approved the final manuscript.

Author details
[1]Department of Mathematics, Faculty of Arts and Sciences, Çankaya University, 06530, Ankara, Turkey. [2]Institute of Space Sciences, P.O. Box, MG-23, R 76900, Magurele-Bucharest, Romania. [3]Department of Medical Research, China Medical University Hospital, China Medical University, Taichung, Taiwan. [4]Department of Electrical and Computer Engineering, Hakim Sabzevari University, Sabzevar, Iran. [5]Department of Physics, College of Sciences, Palestine Technical University, Tulkarm, Palestine. [6]Department of Electrical Engineering, University of Bojnord, P.O. Box, 94531-1339, Bojnord, Iran. [7]Department of Mathematics, Near East University TRNC, Mersin 10, Nicosia, Turkey.

Publisher's Note
Springer Nature remains neutral with regard to jurisdictional claims in published maps and institutional affiliations.

References
1. Ren, H.-P., Bai, C., Kong, Q., Baptista, M.S., Grebogi, C.: A chaotic spread spectrum system for underwater acoustic communication. Phys. A, Stat. Mech. Appl. **478**, 77–92 (2017)
2. Corron, N.J., Hahs, D.W.: A new approach to communications using chaotic signals. IEEE Trans. Circuits Syst. I, Fundam. Theory Appl. **44**(5), 373–382 (1997)
3. Wang, H., Ye, J.-M., Miao, Z.-H., Jonckheere, E.A.: Robust finite-time chaos synchronization of time-delay chaotic systems and its application in secure communication. Trans. Inst. Meas. Control **40**(4), 1177–1187 (2018)
4. Pal, M., Satish, B., Srinivas, K., Rao, P.M., Manimaran, P.: Multifractal detrended cross-correlation analysis of coding and non-coding dna sequences through chaos-game representation. Phys. A, Stat. Mech. Appl. **436**, 596–603 (2015)
5. Hamel, S., Boulkroune, A.: A generalized function projective synchronization scheme for uncertain chaotic systems subject to input nonlinearities. Int. J. Gen. Syst. **45**(6), 689–710 (2016)
6. Grassi, G., Mascolo, S.: Nonlinear observer design to synchronize hyperchaotic systems via a scalar signal. IEEE Trans. Circuits Syst. I, Fundam. Theory Appl. **44**(10), 1011–1014 (1997)
7. Rafikov, M., Balthazar, J.M.: On control and synchronization in chaotic and hyperchaotic systems via linear feedback control. Commun. Nonlinear Sci. Numer. Simul. **13**(7), 1246–1255 (2008)
8. Al-Azzawi, S.F., Aziz, M.M.: Chaos synchronization of nonlinear dynamical systems via a novel analytical approach. Alex. Eng. J. **57**(4), 3493–3500 (2018)
9. Chen, Z., Yuan, X., Yuan, Y., Iu, H.H.-C., Fernando, T.: Parameter identification of chaotic and hyper-chaotic systems using synchronization-based parameter observer. IEEE Trans. Circuits Syst. I, Regul. Pap. **63**(9), 1464–1475 (2016)
10. Batmani, Y.: Chaos control and chaos synchronization using the state-dependent Riccati equation techniques. Trans. Inst. Meas. Control **41**(2), 311–320 (2019)
11. Othman, A.A., Noorani, M., Al-Sawalha, M.M.: Adaptive dual synchronization of chaotic and hyperchaotic systems with fully uncertain parameters. Optik **127**(19), 7852–7864 (2016)
12. Azar, A.T., Serranot, F.E., Vaidyanathan, S.: Sliding mode stabilization and synchronization of fractional order complex chaotic and hyperchaotic systems. In: Mathematical Techniques of Fractional Order Systems, pp. 283–317. Elsevier, Amsterdam (2018)
13. Dongmo, E.D., Ojo, K.S., Woafo, P., Njah, A.N.: Difference synchronization of identical and nonidentical chaotic and hyperchaotic systems of different orders using active backstepping design. J. Comput. Nonlinear Dyn. **13**(5), 051005 (2018)
14. Skinner, J.E.: Low-dimensional chaos in biological systems. Nat. Biotechnol. **12**(6), 596–600 (1994)
15. Vaidyanathan, S.: Global chaos synchronization of the Lotka–Volterra biological systems with four competitive species via active control. Int. J. PharmTech Res. **8**(6), 206–217 (2015)
16. Agarwal, P., Denz, S., Jain, S., Alderremy, A.A., Aly, S.: A new analysis of a partial differential equation arising in biology and population genetics via semi analytical techniques. Phys. A, Stat. Mech. Appl. **542**, 122769 (2020)
17. Sabarathinam, S., Thamilmaran, K.: Controlling of chaos in a tumour growth cancer model: an experimental study. Electron. Lett. **54**(20), 1160–1162 (2018)
18. El-Gohary, A.: Chaos and optimal control of equilibrium states of tumor system with drug. Chaos Solitons Fractals **41**(1), 425–435 (2009)
19. Vaidyanathan, S.: Active control design for the hybrid chaos synchronization of Lotka–Volterra biological systems with four competitive species. Int. J. PharmTech Res. **8**(8), 30–42 (2015)
20. Jajarmi, A., Baleanu, D., Sajjadi, S.S., Asad, J.H.: A new feature of the fractional Euler–Lagrange equations for a coupled oscillator using a nonsingular operator approach. Front. Phys. **7**, 196 (2019)
21. Rezapour, S., Mohammadi, H., Jajarmi, A.: A new mathematical model for Zika virus transmission. Adv. Differ. Equ. **2020**, 589 (2020)
22. Baleanu, D., Jajarmi, A., Sajjadi, S.S., Asad, J.H.: The fractional features of a harmonic oscillator with position-dependent mass. Commun. Theor. Phys. **72**(5), 055002 (2020)
23. Asad, J.H., Baleanu, D., Ghanbari, B., Jajarmi, A., Pirouz, H.M.: Planar system-masses in an equilateral triangle: numerical study within fractional calculus. Comput. Model. Eng. Sci. **124**(3), 953–968 (2020)
24. Jajarmi, A., Baleanu, D.: A new iterative method for the numerical solution of high-order nonlinear fractional boundary value problems. Front. Phys. **8**, 220 (2020)
25. Baleanu, D., Jajarmi, A., Mohammadi, H., Rezapour, S.: A new study on the mathematical modelling of human liver with Caputo–Fabrizio fractional derivative. Chaos Solitons Fractals **134**, 109705 (2020)
26. Agarwal, P., Choi, J.: Fractional calculus operators and their image formulas. J. Korean Math. Soc. **53**(5), 1183–1210 (2016)
27. Rekhviashvili, S.S., Pskhu, A., Agarwal, P., Jain, S.: Application of the fractional oscillator model to describe damped vibrations. Turk. J. Phys. **43**(4), 236–242 (2019)
28. El-Sayed, A.A., Agarwal, P.: Numerical solution of multiterm variable-order fractional differential equations via shifted Legendre polynomials. Math. Methods Appl. Sci. **42**(11), 3978–3991 (2019)

29. Alderremy, A.A., Saad, K.M., Agarwal, P., Aly, S., Jain, S.: Certain new models of the multi space-fractional Gardner equation. Phys. A, Stat. Mech. Appl. **545**, 123806 (2020)

30. Baltaeva, U., Agarwal, P.: Boundary-value problems for the third-order loaded equation with noncharacteristic type-change boundaries. Math. Methods Appl. Sci. **41**(9), 3307–3315 (2018)

31. Wu, G.-C., Baleanu, D., Xie, H.-P., Chen, F.-L.: Chaos synchronization of fractional chaotic maps based on the stability condition. Phys. A, Stat. Mech. Appl. **460**, 374–383 (2016)

32. Boubellouta, A., Zouari, F., Boulkroune, A.: Intelligent fuzzy controller for chaos synchronization of uncertain fractional-order chaotic systems with input nonlinearities. Int. J. Gen. Syst. **48**(3), 211–234 (2019)

33. Al-Khedhairi, A., Matouk, A., Askar, S.: Computations of synchronisation conditions in some fractional-order chaotic and hyperchaotic systems. Pramana **92**(5), 72 (2019)

34. Sajjadi, S.S., Baleanu, D., Jajarmi, A., Pirouz, H.M.: A new adaptive synchronization and hyperchaos control of a biological snap oscillator. Chaos Solitons Fractals **138**, 109919 (2020)

35. Nazari, S., Heydari, A., Khaligh, J.: Modified modeling of the heart by applying nonlinear oscillators and designing proper control signal. Appl. Math. **4**(7), 972–978 (2013)

36. Van Der Pol, B., Van Der Mark, J.: Lxxii. The heartbeat considered as a relaxation oscillation, and an electrical model of the heart. London, Edinburgh, Dublin Philos. Mag. J. Sci. **6**(38), 763–775 (1928)

37. Mainardi, F.: Fractional relaxation-oscillation and fractional diffusion-wave phenomena. Chaos Solitons Fractals **7**(9), 1461–1477 (1996)

38. Caputo, M.: Linear models of dissipation whose q is almost frequency independent. Ann. Geophys. **19**(4), 383–393 (1966)

39. Baleanu, D., Jajarmi, A., Sajjadi, S.S., Mozyrska, D.: A new fractional model and optimal control of a tumor-immune surveillance with non-singular derivative operator. Chaos, Interdiscip. J. Nonlinear Sci. **29**(8), 083127 (2019)

40. Diethelm, K., Freed, A.D.: The fracpece subroutine for the numerical solution of differential equations of fractional order. Forsch. Wissenschaft. Rech. **1999**, 57–71 (1998)

41. Matouk, A.E.: Stability conditions, hyperchaos and control in a novel fractional order hyperchaotic system. Phys. Lett. **373**(25), 2166–2173 (2009)

42. Kirk, D.E.: Optimal Control Theory: An Introduction. Courier Corporation (2004)

43. Shojaei, K., Chatraei, A.: A saturating extension of an output feedback controller for internally damped Euler–Lagrange systems. Asian J. Control **17**(6), 2175–2187 (2015)

44. Jajarmi, A., Hajipour, M.: An efficient recursive shooting method for the optimal control of time-varying systems with state time-delay. Appl. Math. Model. **40**(4), 2756–2769 (2016)

45. Jajarmi, A., Pariz, N., Effati, S., Vahidian Kamyad, A.: Infinite horizon optimal control for nonlinear interconnected large-scale dynamical systems with an application to optimal attitude control. Asian J. Control **14**(5), 1239–1250 (2012)

46. Effati, S., Saberi Nik, H., Jajarmi, A.: Hyperchaos control of the hyperchaotic Chen system by optimal control design. Nonlinear Dyn. **73**(1–2), 499–508 (2013)

47. Jajarmi, A., Baleanu, D.: On the fractional optimal control problems with a general derivative operator. Asian J. Control **23**(2), 1062–1071 (2021)

48. Jajarmi, A., Yusuf, A., Baleanu, D., Inc, M.: A new fractional HRSV model and its optimal control: a non-singular operator approach. Phys. A, Stat. Mech. Appl. **547**, 123860 (2020)

49. Yıldız, T.A., Jajarmi, A., Yıldız, B., Baleanu, D.: New aspects of time fractional optimal control problems within operators with nonsingular kernel. Discrete Contin. Dyn. Syst., Ser. S **13**(3), 407–428 (2020)